HHS Public Access

Author manuscript

Anal Chem. Author manuscript; available in PMC 2017 September 06.

Published in final edited form as:

Anal Chem. 2016 September 06; 88(17): 8827–8834. doi:10.1021/acs.analchem.6b01945.

Fast photochemical oxidation of proteins (FPOP) maps the topology of intrinsic membrane proteins: light-harvesting complex 2 (LH2) in a Nanodisc

Yue Lu[a,b], **Hao Zhang**[a,b], **Dariusz M. Niedzwiedzki**[b], **Jing Jiang**[b,c], **Robert E. Blankenship**[a,b,d,*], and **Michael L. Gross**[a,b,*]

[a]Department of Chemistry, Washington University in St. Louis, St. Louis, MO 63130, USA

[b]Photosynthetic Antenna Research Center, Washington University in St. Louis, St. Louis, Missouri 63130, United States

[c]Department of Energy, Environmental and Chemical Engineering, Washington University in St. Louis, St. Louis, MO 63130, USA

[d]Department of Biology, Washington University in St. Louis, St. Louis, MO 63130, USA

Abstract

Although membrane proteins are crucial participants in photosynthesis and other biological processes, many lack high-resolution structures. Prior to achieving a high-resolution structure, we are investigating whether MS-based footprinting can provide coarse-grained protein structure by following structural changes that occur upon ligand binding, pH change, and membrane binding. Our platform probes topology and conformation of membrane proteins by combining MS-based footprinting, specifically fast photochemical oxidation of proteins (FPOP), and lipid Nanodiscs, which more similar to the native membrane environment than are the widely used detergent micelles. We describe here results that show a protein's outer membrane regions are more heavily footprinted by OH radicals whereas the regions spanning the lipid bilayer remain inert to the labeling. Nanodiscs generally exhibit more protection of membrane proteins compared to detergent micelles and less shielding to those protein residues that exist outside the membrane. The combination of immobilizing the protein in Nanodiscs and footprinting with the FPOP approach is a feasible approach to map extra-membrane protein surfaces, even at the amino-acid level, and to illuminate intrinsic membrane protein topology.

Graphical abstract

Corresponding authors: Michael L. Gross, mgross@wustl.edu, Robert E. Blankenship, blankenship@wustl.edu.

Associated Content

Supporting Information

The Supporting Information is available free of charge on the ACS Publications website.

Methods include preparation of Nanodisc and characterizations of Nanodisc (steady-state spectroscopy, time-resolved fluorescent, dynamic light scattering and Data analysis); Steady-state absorption spectrum of LH2 in detergent micelles and Nanodiscs; Time-resolved fluorescence spectrum of LH2 in detergent and Nanodisc; Dynamic light scattering of empty-nanodisc and LH2-Nanodiscs; Coverage map of LH2; Oxidation level of [Leu5]-Enkephalin YGGFL in detergent micelle/Nanodisc environment; Corresponding amino acids of Mets (Rb. sphaeroides) shown in PDB 1NKZ; Sequence alignments of LH2; EIC of m/z = 649.3074 (PAYYQGSAAVAAE); MS/MS fragmentation spectrums of different peptides; Measurement of solvent inaccessible region of LH2 by Pymol; Oxidation level of N-terminal peptides from both β subunit.

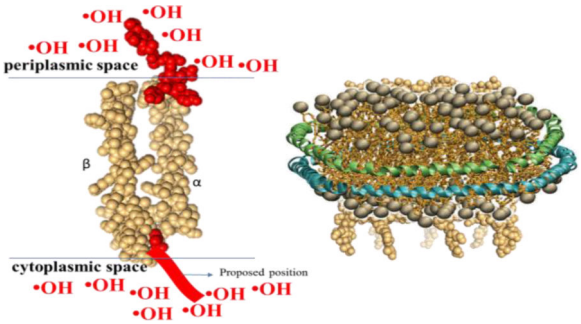

Introduction

Membrane proteins are involved in crucial cellular functions, including photosynthesis[1], respiration[2] and signal transduction[3]. They represent ~30% of open reading frames[4] of many genomes, and an increasing number of them are important drug targets.[5] One way membrane proteins perform their functions is via interaction with other molecules or with themselves to undergo conformational changes important in signaling, for example. Membrane proteins are highly flexible and dynamic, enabling them to perform different tasks with high efficiency but making structure determination difficult. Membrane protein structures are notoriously difficult to resolve compared to water-soluble proteins.[6] Because membrane proteins are hydrophobic, they need detergent for solubilizing and stabilizing them in water. Detergents, however, can affect protein conformation and hinder protein interaction with other molecules. Compared to the large number of soluble proteins, high-resolution structures are available only for a small fraction of membrane proteins.[7]

Various detergents are used to extract membrane proteins from their native lipid bilayer and to solubilize, stabilize and enclose them in micelles.[8] Unfortunately, detergents are not an ideal mimic of cellular environment. The different micelle sizes and curvature restrictions compromise protein stability and, in some cases, proper protein functioning.[9] In addition, an excess micellar phase may interfere with the interaction with other molecules and pose challenges for analytical methods. To overcome these problems, researchers reconstitute membrane protein in monolayers, bicelles, and liposomes.

One approach that provides a better mimic of a native environment and controllable stoichiometry of target membrane protein is the lipid-protein Nanodisc.[10] Here, two membrane scaffold proteins (MSP) form a double belt to enclose a lipid bilayer and form a water-soluble disc into which target membrane proteins can be incorporated. Under self-assembly conditions, the oligomeric state of a target protein and the nature of the lipids included in the bilayer can be controlled, allowing a membrane protein to be probed from both the cytoplasmic and the periplasmic sides of the membrane. Thus, a Nanodisc provides a simple and robust means for rendering target membrane proteins in aqueous buffer while keeping the protein in a native-like bilayer environment.[11]

Membrane topology can be viewed as “an important halfway house between the amino-acid sequence and the fully folded three-dimensional structure”.[12] Individual transmembrane helices can insert into a lipid bilayer in different ways, and because the proteins are

dynamic, they can change conformation and position. Various mass spectrometry (MS)-based labeling methods are now being widely adopted to study those issues; one of them, cross-linking, has become dominant in probing protein-protein interactions.[13] ther labeling reagents (e.g., carbodiimide compounds[14]), can be also used to elucidate the structure of membrane protein. MS-based footprinting (hydrogen/deuterium exchange (HDX) and reactions with •OH and other radicals) is complementary. These approaches label most of the amino acids to illuminate protein-protein, and protein-ligand interactions.[15] HDX is widely used for soluble proteins, and the extent of exchange reports on H bonding and solvent accessibility of the protein backbone.[16–17] HDX can be effective for membrane proteins when conducted in the presence of detergent micelles provided the protocol includes fast isolation, good digestion efficiency, and solubility of materials.[18–19] Footprinting, done with the FPOP platform, can label amino acids with OH radicals produced by photolysing hydrogen peroxide. The amino-acid reactivity with hydroxyl radicals is broad-based although the reactivity with amino acid side chains can vary by three orders of magnitude.[20] The dominant product is a +16 adduct, but there are other pathways and products. FPOP probes solvent accessibility of different regions of proteins in a fraction of a second and at the amino acid level.[21] The labeling is carefully controlled so that every fraction or plug of a flowing protein buffer solution is labeled only once. Compared to the more widely used HDX, the irreversible labeling provides flexibility in digestion as there is no concern for back exchange and good potential for general membrane protein studies, as lipid removal prior to MS analysis is relatively easily accomplished.

To our knowledge, only a few methodologies regarding oxidatively labeling of membrane proteins described so far. Sze et al.[22] adopted a Fenton reaction to oxidize the outer membrane of porins and revealed the voltage gating of the porin OmpF *in vivo*. Konermann et al.[23] carried out the first FPOP oxidative labeling of a membrane protein, bacteriorhodopsin, in a natural lipid bilayer environment. They found that oxidative modification of methionines located in solvent-accessible loops are highly oxidized compared to those located in the transmembrane regions, taking advantage of a protein that is rich in Met, which is highly susceptible to oxidative modifications. A subsequent study by that group revealed the conformational change of denatured bacteriorhodopsin in SDS compared to the native state.[24]

More recently, Chance used X-ray radiolytic footprinting with •OH to study structural water and conformational change of membrane proteins.[25–26] For example, after dissolving rhodopsin in detergent, radiolysis-produced •OH labeled both solvent-accessible and solvent-inaccessible regions. The labeling of solvent-inaccessible regions may be due to tightly bound structural water molecules that are ionized by the radiation, produce •OH, and label nearby residues.[27] The approach elucidates *in vivo* structural dynamics in integral membrane protein by •OH reactions.

The successful reconstitution of a variety of membrane proteins into Nanodiscs[28–30] and characterized by other biophysical methods allows us to seek higher resolution structural information to complement data on the size and activity of membrane proteins. High motivation exists for this goal because no crystal structure exists for many membrane proteins including the LH2 of interest here. One approach is footprinting of target membrane

proteins embedded in Nanodiscs by using HDX coupled with MS. Jorgenson, Rand, Engen and coworkers probed the conformational analysis of γ-glutamyl carboxylase by in Nanodiscs by HDX MS.[31] Subsequently, Jorgenson, Stafford and coworkers[32] investigated binding of γ-glutamyl carboxylase to a propeptide, employing good separation and HDX MS. Recently, Adkins and coworkers[33] studied the membrane interactions, ligand-dependent dynamics, and stability of cytochrome P450 in Nanodiscs by HDX MS. In these HDX studies, it is required to disassemble rapidly the Nanodisc and remove the excess lipid from solution prior to MS analysis while minimizing back exchange, which can be a nagging problem.

Another approach, which we describe here, is MS-based FPOP footprinting of a membrane protein complex in a near-native environment. As a model protein, we used the light-harvesting complex 2 (LH2) from *Rhodobacter (Rb.) sphaeroides*, an intrinsic membrane protein with ~18 transmembrane helices[34] We used Nanodiscs to "house" the LH2 in aqueous buffer prior to and during labeling by hydroxyl radicals. Unlike many other proteins studied in Nanodiscs, LH2 contains number of bound pigments that guide the insertion and provide assurance that the protein is inserted in its native state. We compared the solvent accessibility of LH2 from FPOP with that in detergent micelles and identified labeling at the residue level. Our results show that Nanodiscs generally provide a better protection of the transmembrane core region of protein and less shielding for the outer membrane region. The purpose is to develop a method for biophysical studies of membrane proteins.

Methods

Footprinting of Nanodisc-LH2 and detergent micelle-embedded LH2

The LH2 concentration was estimated by using the molar absorptivity of B850 bacteriochlorophyll *a*[35], and the MSP concentration was calculated according to the predicted molar absorptivity at 280 nm and used for the following experiments.[36] The LH2-Nanodisc sample was dissolved in PBS buffer to the specifications: 2 μM of Nanodisc-LH2, 350 μM of histidine, 5 μM of [leu5]-enkephalin (reporter peptide), and 20 mM of H_2O_2. The LH2 dissolved in PBS buffer containing 0.02% DDM, 2 μM of LH2, 2 μM of MSP, 350 μM histidine, 5 μM of [leu5]-enkephalin (reporter peptide), and 20 mM H_2O_2. To minimize any pre-oxidation by H_2O_2, it was added immediately into the solution prior to loading the syringe pump. The FPOP experiment was performed as previously described.[37] The energy of the KrF excimer laser (GAM Laser Inc., Orlando, FL) was adjusted to 22.3 mJ, and sample flow rate was 22 μL/min to ensure a 20% exclusion volume. After laser-induced labeling, each sample was collected in a vial containing 10 mM catalase and 20 mM Met to eliminate leftover H_2O_2. Control samples for both Nanodisc- and detergent-LH2 were handled in the same manner without laser irradiation. All experiments were performed in triplicate. For each collection, the buffer was divided into two portions. Formic acid (1%) was added to one portion prior to desalting with a Sep pak C18 (Waters Inco., Milford, MA). The other portion was precipitated with acetone and dissolved in buffer containing 100 mM Tris, 1 mM $CaCl_2$, and 0.02% RapiGest SF (Waters Inco., Milford, MA). Digestion was at 37 °C for 1 h with chymotrypsin (Promega Corporation, Madison, WI) and subsequently quenched by FA (1%).

MS analysis

Peptide mixtures were trapped by a guard column (Acclaim PepMap100, 100 μm × 2 cm, C18, 5 μm, 100 Å; Thermo Fisher Scientific, Breda, Netherlands) and then fractionated on a custom-packed Magic C18 reversed-phase column. The MS analysis was with a Thermo Scientific™ Q Exactive™ hybrid quadrupole-Orbitrap mass spectrometer (Thermo Fisher Scientific, Bremen Germany). Peptides were eluted with a 85 min, 250 nL/min gradient coupled to the nanospray source. A 50 min, 250 nL/min gradient was adopted for the reporter-peptide analysis. The default charge state was 2, and the scan range was from *m/z* 380-1500. Mass spectra were obtained at high mass resolving power (70,000, FWHM at *m/z* 200) and the top 15 most abundant ions corresponding to eluting peptides per scan were submitted to CID in the ion trap, with charge-state rejection of unassigned and >8 ions enabled. Precursor ions were added to a dynamic exclusion list for 8 s to ensure good sampling of each elution peak.

Data analysis

Details of data processing are in supplementary information.

Sequence alignment, topology prediction and homology modeling

Sequence alignment of LH2 from different purple bacteria was performed by an online web server.[38] The TOPCONS web server was adopted for prediction of LH2 topology.[39] Homology models of LH2 from *Rb. sphaeroides* were generated, as previously described.[40] The heterodimer models (α and β) were based on PDB 1NKZ and processed by Pymol[41] (The PyMOL Molecular Graphics System, Version 1.7.4 Schrödinger, LLC.).

Results and discussion

Characterization of the Nanodisc containing LH2

The model membrane protein in this study is LH2, a protein complex belonging to the photosynthetic antenna family whose primary function is to harvest light and transfer absorbed energy to a reaction center. It is important to characterize the protein in Nanodiscs and detergent prior to footprinting to insure that our comparisons are valid and that the Nanodisc indeed contains the intact complex. An advantage of using LH2 is the Nanodisc-protein can be convincingly characterized by absorption and fluorescence spectroscopies. Ideally, LH2 preparations in Nanodiscs and detergent media should show identical absorption spectra with characteristic well-developed and resolved electronic absorption bands for bound pigments (i.e., B800 and B850 bands at 800 and 850 nm associated with bacteriochlorophyll *a*, and carotenoid (spheroidene) absorption band between 480 and 515 nm). This essential analysis shows that the pigment environments are not fundamentally altered in the two preparations (Figure S1).

In addition, the intact LH2 complex can be probed by time-resolved fluorescence using the B850 emission. The B850 fluorescence decay lifetime of this LH2 complex is typically ~ 1 ns[42], and any significant variation of this value will indicate perturbation of the B850 bacteriochlorophyll *a* array. Furthermore, different excitonic coupling in the B850 exciton will alter the rate of radiative decay. Alternatively, a significant reduction of fluorescence

lifetime of the Nanodisc-LH2 would indicate that the Nanodisc bundles more than one LH2 complex and allows formation of oligomeric LH2 structures. As shown in Figure S2, however, the B850 fluorescence lifetimes are essentially the same for both preparations and fit the expected time range for monomeric and not structurally deficient or altered LH2. To add certainty, we also used the A850/A280 ratio as a marker of the LH2 purity. The ratio for LH2 in detergent (3.05) should be higher than in in the Nanodiscs (2.34) because the MSP also contributes to the absorption at 280 nm and lowers the ratio. Furthermore, a calculation based on molar absorptivity indicates that the Nanodisc contains one LH2 complex and that some (~75%) of empty nanodisc is also present.

To complete the characterization of the protein preparation, we used dynamic light scattering (DLS) to characterize rapidly the particle size of the Nanodisc.[43] The homogeneity of empty- and LH2-embeded Nanodiscs is revealed by the size distribution (Figure S3). The result (diameter ~10 nm) is consistent with a previous report[44] and demonstrates that the Nanodisc-LH2 is slightly larger compared to the empty-Nanodisc. This perturbation is probably caused by expansion of the disc induced by the LH2 residing in its middle, and it is consistent with a previous report that shows that addition of a target membrane protein into a Nanodisc slightly enlarges its dimensions.[45]

Feasibility of FPOP to membrane proteins

We are advocating irreversible labeling with the hydroxyl radical to permit, prior to the MS analysis, easier lipid removal such as acetone precipitation, chloroform/methanol extraction, and other forms of off-line desalting by use of reversed-phase cartridges. Indeed, we adopted acetone precipitation, and we could remove most of the lipid after processing. Moreover, we could obtain complete coverage (100%) in the digestion of the α and β subunits in LH2 (Figure S4) and extend the analysis from the peptide to the amino-acid residue level in some cases. Our results show that the regions that are likely to be in the cytoplasmic or periplasmic space undergo a higher extent of oxidative labeling compared to the regions of the protein deeply embedded in the Nanodisc (Figure 1). The MSP proteins that wrap around the lipid bilayer also become labeled to different extents for different regions.

Membrane protein in detergent micelle vs. Nanodisc

Because both lipids and detergents are prone to oxidative modifications by •OH[46–47], we measured the hydroxyl radical reactivity in the two environments normalized to the labeling yield of a reporter peptide (i.e., the five amino-acid leu enkephalin)[48]. In this way, we can compensate for any differences in protein reactivity introduced by changing from detergent to Nanodisc. We found that the oxidation level of the reporter peptide in Nanodiscs is 1.67 times greater than with the DDM micelles under the same experimental conditions (Figure S5). Due to the lack of high resolution structure, we then used homology modeling with the known structure of LH2 from *Rps. acidophila* [49] and obtained a result with the high certainty (99.9%) to assist the discussion of the results.

Although large amounts of lipids are present in the Nanodisc, their alkyl tails are embedded and not highly available for reaction with free radicals. Coarse-grain molecular dynamics simulations reveal that the lipids in the Nanodisc have higher acyl tail order than lipids in a

lamellar bilayer phase.[50] The detergent, however, exists as a monomer at low concentration, and when its concentration is increased above the critical micelle concentration (CMC), it self-associates to form non-covalent micelles. Although a spherical detergent micelle is often viewed as uniformly packed, they are not, and the octyl glucoside micelles contain a distribution of surfactant molecules. Instead of a static shape, as usually assumed, those different size micelles fluctuate between spherical and near-ellipsoidal shapes.[51] And not all hydrophobic tails are buried or point toward the center of the micelle; rather the micelle surface is rough and heterogeneous. Furthermore, the state of detergent micelles and of detergent-protein micelles is relatively dynamic, undergoing rapid exchange of detergent and solvent.[52] Thus, a detergent is more likely to quench •OH than a Nanodisc.

Considering now the protein complex in a Nanodisc, we find, as expected, that the solvent-exposed terminal regions of LH2 undergo greater oxidative modification than the transmembrane regions. (Figure 1). Although this is the case for both the detergent and the Nanodisc, we expect that the hydrophobic regions of a membrane protein will be protected less in a detergent micelle than in Nanodiscs, and this is seen for all regions of LH2 where the oxidation level is larger in the presence of detergent micelles than of Nanodiscs. Nevertheless, the overall reactivity trends are similar, suggesting that detergent micelles do provide a similar environment to the lipid bilayer. A previous study shows that detergent molecules in a globular micelle can exchange over hundreds of nanoseconds with detergent molecules in a micelle bound to a protein.[53] For example, the dynamic fluctuations of OmpA protein are 1.5 times greater in the micellar environment than in the lipid bilayer, and this increased overall mobility may be attributed to the increased diffusion properties and reduced packing of detergent molecules.[54] The differences we observed are in accord with those results, suggesting that membrane proteins in detergent micelles have more flexibility and solvent accessibility compared to in a lipid Nanodisc. For the methionine residues located in the transmembrane region of LH2, the Nanodisc affords even more protection than detergent micelles. This region of LH2 is embedded in the lipid bilayer of a Nanodisc but only closely associated with hydrophobic tails in the detergent (Figure S4).

Methionine as a marker in membrane protein labeling by FPOP

A previous study of bacteriorhodopsin reported extensive oxidation of only methionines located in its solvent-accessible loops.[24] For LH2 in our study, Met is also relatively reactive, but the protein reactivity occurs on many residues besides Met. For each heterodimer (α and β) composing the ring of LH2, there are three Mets (Figure S7). One is probably in the transmembrane region, and the other two are near the N-terminus. LH2 in a lipid bilayer exhibits higher protection for the regions containing Met compared to those in a detergent micelle. According to the homology modeling, the N-terminal Met of the α subunit is not protruding into the outer region of the membrane but instead is bent toward the inner region of a lipid bilayer[40] where it coordinates the central Mg^{2+} ion of a nearby bacteriochlorophyll *a*, and preserves the planar conformation of the pigment molecule.

The axial coordination of a central Mg^{2+} ion is crucial for all the photosynthetic chlorophyll-proteins, in terms of both structure and function.[55] A carboxyl modified Met1 of the α subunit from *Rhodopseudomonas (Rps.) acidophila* is ligated to Mg^{2+} of B800[49] whereas

for *Rhodospirillum (Rs.) molischianum*[56], the corresponding ligand is Asp6. For both these structures, the N-terminal regions of the α subunits exist as a loop structure but are closely associated with the transmembrane regions owing to its coordination with B800. In our homology model, the N-terminal of α subunit of the LH2 from *Rb. sphaeroides* is also closely associated with the transmembrane region. (Figure 2 and see figure S6) The Met located in the transmembrane region of the protein shows a similar oxidative modification to the one located on the N-terminal of the α subunit. The first few amino acids on the N-terminal end of the β subunit are not covered in the homology model (see Figure S7). We suggest this Met is pushed out of the membrane and undergoes relatively high oxidative modification. As a reference, the methionine-containing peptides from the MSP of the Nanodisc show a 0.15-0.60 range of oxidation. To provide a coarse-grained view of the locations of those three Mets in the ring structure, the corresponding residues in PDB 1NKZ are labeled in Supplementary figure. We conclude that the extent of oxidative modification of the highly reactive Met is a good marker for the topology of transmembrane proteins on the FPOP platform.

Locating the membrane protein in the lipid bilayer

Membrane proteins are closely associated with lipid bilayers, and their integral transmembrane domains are more deeply embedded in those membranes than are exterior regions. It is intriguing to probe the interaction of lipid bilayer with different domains of membrane proteins. The lipid hydrophobic tails are closely associated with the LH2 hydrophobic transmembrane domains, and their lengths determine the thickness of the membrane core (typically ~ 3 nm). The thickness of the polar head of lipids on each side is ~ 1.5 nm.[57–58] Siuda et al.[59] observed that the Nanodisc thickness is smaller near the MSP double belt, owing to the perturbation from boundary lipids. The average thickness of MSP1E3, which is the MSP we used for the LH2-Nanodisc, obtained by applying small-angle X-ray scattering (SAXS), is 4.6 nm. Previous studies showed the Stokes diameter of MSP1E3 is 12.1 nm, whereas SAXS gives a value of 12.8 nm.[10] LH2, mapped by atomic force microscopy, shows average center-to-center distances between complexes within the dimer as 7.7 nm.[60] The above values show that although the LH2 has a relatively large transmembrane domain, it could be positioned in the middle of the MSP1E3D1 Nanodisc. Those values also strongly suggest that only a single LH2 complex can be incorporated into the Nanodisc.

Although an increasing number of high-resolution crystal structures of membrane proteins are published every year, it is necessary to picture the topology of membrane protein sitting in the dynamic membrane bilayer. To do this, we adopted the TOPCONS web server [61] for a consensus prediction of the structural and functional features, membrane-inside and outside (i and o, respectively). In addition, we used a biological hydrophobicity scale to predict the free energy of membrane insertion centered on each position in the sequence.[39] Experimental data, however, are needed to confirm the topology and conformation of membrane proteins. Oxidative labeling shows that the terminal ends of the two transmembrane helices are more heavily solvent-accessible than are the integral regions. The oxidative modification levels are generally in accord with the free-energy trends. For transmembrane regions, little or no oxidative modification occurs. Further, LH2 in the

Nanodisc shows a lower level of oxidation compared to the one in detergent, suggesting better protection of LH2 in a lipid bilayer (Figure 1).

The Met in the N-terminal end of the α subunit, as discussed above, is pointed inward to coordinate a pigment molecule. Thus, the oxidation level of this Met is not high compared to the other Met residues in the protein assembly (Figure 2). The C-terminal end of the α subunit is highly modified even though no highly reactive methionine is present (Figure 1a). This region, as modeled with 99.9% confidence to the crystal structure of the LH2 from *Rps. acidophila*, shows a helix-loop sticking out of the "ball" structure (Figure 3). This region has an extended conformation that passes between the β-chains of the neighboring heterodimers, and the large occupancy volume indicates high flexibility.[49] The extracted ion chromatogram (EIC) of the oxidized form (+ 16) shows one major and two minor peaks (Figure S8). The product-ion spectra (Figure S9a-e) reveal that the first two minor peaks represent the peptide with oxidatively modified Tyr, Ser and Val, and the major peak represents the peptide with an oxidized Pro. Because the elution time for peptides containing oxidized Tyr, Ser or Val are overlapping, we cannot differentiate the modification extents of those residues in detergent or in the Nanodisc. The rate constants of Pro, Ser and Val with •OH are of the same order of magnitude but an order of magnitude lower than that for Tyr.[19] The high oxidative extent of Pro and low level of Tyr should be related to the protein conformation of this region. The 2.0 Å crystal structure of the LH2 from the template shows that the glucoside head groups of the rhodopsin glucoside carotenoid molecule (RG1) are located at the cytoplasmic surface whereas the second carotenoid (RG2) is at the periplasmic surface (Figure 4).[49] Raman scattering, however, shows no bands that could be attributed to RG2.[62] Later, the authors claimed that this RG2 site is actually occupied by a mix of BOG and LDAO molecules, owing to incomplete detergent exchange. This RG2 was located adjacent to the Tyr residues, as shown in Figure 4. Our results also suggest that this Tyr site is relatively solvent-inaccessible owing to its association with detergents/lipids. The crystal structure shows Pro is facing inward and the other residues are either shielded by the detergent/lipid molecules (Tyr-Tyr in PDB 1NKZ, Tyr-Tyr in the homology model) or adjacent to the C-terminal end of the β subunit (Gly in PDB 1NKZ and Ser in the homology model) with the exception of valine (Figure 4a-c). We propose that the association of transmembrane helices with detergents/lipids in the hole or center of the LH2 ring complex is different than outside, similar to the lipids adjoining the MSP in the Nanodisc where the thickness of the disc is smaller. This may be a result of distorted packing of the lipids to minimize any hydrophobic mismatch at the protein-lipid interface.[59, 63] It is interesting that the Pro exhibits lower oxidative modification in Nanodiscs, which is consistent with the behavior of other peptides/residues in LH2. Other residues (Tyr, Ser and Val) in this peptide, however, exhibit slightly higher levels of oxidation in Nanodiscs than in detergent, suggesting that the lipids provide better protection of proline compared to the detergent micelle, while the other residues are slightly more exposed in the lipid bilayer (Figure 4d). The detergent micelle might hinder the solvent accessibility of a number of residues on the surface of the C-terminal end of the α subunit, whereas relatively more regularly packed lipids in the Nanodiscs exhibit lesser blocking.

The C-terminal loop domain of the β subunit (AAAATPWLG), does not extend from the membrane but more likely exists at a water/lipid interface and bends inward (Figure 3),

consistent with its low oxidative labeling (Figure 1b). Although Trp, a highly reactive residue with •OH, is present in this subunit, no prominent oxidative modification occurs for it (Figure 1b). MS/MS shows only the terminal Pro, Trp and Leu are oxidatively modified (see Figure S9f-h) but not Gly, which is inert to FPOP.

The consensus from TOPCON also indicates that the N-terminal end is much less hydrophobic than the C-terminal end. The former contains an N-terminal Met that undergoes the highest oxidative modification of all the Mets (Figure 2). This Met in the β subunit has higher solvent-accessibility than the others. Although this region is not covered in our homology model[40], it may exist, on the basis of LH2 from *Rps. acidophila*[49], as an elongated peptide region attached to the homology model (Figure S7). This region extends beyond the membrane and has good solvent accessibility (Figure 1b). The remaining part of the LH2 is approximately 5 nm in length (Pymol), a length that is nearly the same as the width of the Nanodisc (4.6 nm)[59] (Figure S10). On the basis of the above discussion, we can propose a borderline between the solvent accessible domains and the domains that are embedded in hydrophobic tails of lipids (Figure 5).

The final question we want to address is the topology difference of the two β subunits; this topology could be crucial for the function of LH2.[64] The function of the second copy of β subunits was previously investigated by amplifying and cloning the Puc2BA operon of *Rb. sphaeroides*. The resulting LH2 is spectroscopically distinct from the Puc1BA encoded LH2 with a blue-shifted B850 absorption band at 846 nm.[65] Another study found that Puc2AB-encoded LH2 is predominant under high light and as it acclimates to low light.[66] To assess the solvent accessibility and topology of the two β subunits, we compared the oxidation levels of the N-terminal peptides from the subunits. We used the longer peptide on the N terminal end for this comparison as the signal intensity of the shorter β2 peptide was too low. Because a highly reactive Met is present on the N-terminal end of the β1 subunit and not on the β2 end, it is difficult to make a fair comparison. No oxidation of Val and Trp occurs for the β1 subunit, whereas ~ 6% of oxidative modification of Val or Trp occurs in the β2 subunit (Figure S9i-l and Figure S11). This result suggests that the regions adjacent to Val and Trp of the β2 subunit are more exposed to the cytoplasmic space than is β1. Although the roles of the two copies of β are still not fully understood, this study provides another perspective.

Conclusions

We describe here an MS-based platform to map the topology and conformation of an intrinsic membrane protein complex. To the best of our knowledge, this is the largest transmembrane assembly successfully inserted into Nanodiscs. Although this large protein complex has overall ~18 transmembrane helices and most are embedded in the lipid bilayer, there is only one transmembrane helix for each subunit. The outer-membrane structures are short and have little higher order structure, affording an opportunity to understand steric shielding at the interface of lipid/water.

We probed the LH2 topology and conformation in both lipid Nanodics and detergent micelles. The oxidative-modification extents of peptides/residues show that Nanodiscs

generally provide better protection for LH2 than do detergent micelles. For residues located at the membrane interface, there is also less shielding in the Nanodisc system. Nevertheless, Met residues show high modification propensity and may be a good marker for comparing solvent accessibility of different regions. Isolation of protein from lipids prior to MS analysis is less constrained with FPOP footprinting than with HDX. Lipid Nanodiscs offer accessibility from both sides of the membrane and the opportunity to assess topology and conformation of membrane protein in a near native-state. Thus, a platform involving proteins inserted in a Nanodisc and their footprinting by FPOP is promising for studying membrane-protein topology. It offers the opportunity to determine interactions of membrane protein with other molecules, conformational changes of membrane proteins induced by various factors, and the lipid influence on membrane proteins. The ultimate goal is to use FPOP or other footprinting for in-cell footprinting.

Jones and coworkers[67] successfully did the first in-cell FPOP labeling and found oxidative modification of proteins, including several membrane proteins, within various subcellular compartments. The in-vitro membrane-protein footprinting in in a relevant Nanodisk reported here, however, is necessary to answer systematically detailed biophysical questions as a preamble to in-cell footprinting, and this is the purpose of our report. Although detergent micelles are the most widely used medium, Nanodiscs are a better mimic as they provide a more native-like lipid bilayer environment. To address a membrane protein in those two popular vehicles, the FPOP platform can offer a zoom-in picture of many of the amino-acid residues of the membrane protein, setting the stage for later in-cell studies.

Supplementary Material

Refer to Web version on PubMed Central for supplementary material.

Acknowledgments

We would like to thank Sligar lab for providing the MSP protein in our initial studies and for the helpful advice of Yelena V. Grinkova and Michael T. Marty.

Funding

This research is funded by the Photosynthetic Antenna Research Center (PARC), an Energy Frontier Research Center funded by the DOE, Office of Science, Office of Basic Energy Sciences under Award Number DE-SC 0001035 and National Institute of General Medical Science (NIGMS of the NIH) under Grant Number: 8 P41 GM103422. YL, HZ, DN, JJ and sample preparation were supported by the DOE grant. Mass spectrometry instrumentation and resources were provided by the DOE and NIH grants.

References

1. Blankenship, RE. Molecular Mechanisms of Photosynthesis. Wiley; 2002.
2. Krause F. Electrophoresis. 2006; 27(13):2759–2781. [PubMed: 16817166]
3. Pan J, Misamore MJ, Wang Q, Snell WJ. Traffic. 2003; 4(7):452–459. [PubMed: 12795690]
4. Wallin E, Heijne GV. Protein Sci. 1998; 7(4):1029–1038. [PubMed: 9568909]
5. Grimm D, Bauer J, Pietsch J, Infanger M, Eucker J, Eilles C, Schoenberger. J. Curr. Med. Chem. 18(2):176–190.
6. Carpenter EP, Beis K, Cameron AD, Iwata S. Curr. Opin. Struct. Biol. 2008; 18(5):581–586. [PubMed: 18674618]
7. http://blanco.biomol.uci.edu/mpstruc/

8. Seddon AM, Curnow P, Booth PJ. Biochim. Biophys. Acta, Biomembr. 2004; 1666(1–2):105–117.
9. Rice AJ, Alvarez FJD, Davidson AL, Pinkett HW. Channels. 2014; 8(4):327–333. [PubMed: 24852576]
10. Denisov IG, Grinkova YV, Lazarides AA, Sligar SG. J. Am. Chem. Soc. 2004; 126(11):3477–3487. [PubMed: 15025475]
11. Shen H-H, Lithgow T, Martin L. Int. J. Mol. Sci. 2013; 14(1):1589. [PubMed: 23344058]
12. von Heijne G. Nat. Rev. Mol. Cell. Biol. 2006; 7(12):909–918. [PubMed: 17139331]
13. Rappsilber J. J. Struct. Biol. 2011; 173(3):530–540. [PubMed: 21029779]
14. Weinglass AB, Whitelegge JP, Hu Y, Verner GE, Faull KF, Kaback HR. EMBO J. 2003; 22(7):1467–1477. [PubMed: 12660154]
15. Rajabi K, Ashcroft AE, Radford SE. Methods. 2015; 89:13–21. [PubMed: 25782628]
16. Hoofnagle, Andrew N.; Resing, Katheryn A.; Ahn, NG. Annu Rev Biophys. 2003; 32(1):1–25.
17. Bennett BC, Gardberg AS, Blair MD, Dealwis CG. Acta Crystallogr., Sect. D: Biol. Crystallogr. 2008; 64(7):764–783.
18. Zhang X, Chien EYT, Chalmers MJ, Pascal BD, Gatchalian J, Stevens RC, Griffin PR. Anal. Chem. 2010; 82(3):1100–1108. [PubMed: 20058880]
19. Busenlehner LS, Salomonsson L, Brzezinski P, Armstrong RN. Proc. Natl. Acad. Sci. U.S.A. 2006; 103(42):15398–15403. [PubMed: 17023543]
20. Xu G, Chance MR. Chem. Rev. 2007; 107(8):3514–3543. [PubMed: 17683160]
21. Niu B, Zhang H, Giblin D, Rempel DL, Gross ML. J. Am. Soc. Mass Spectrom. 2015; 26(5):843–846. [PubMed: 25712620]
22. Zhu Y, Guo T, Park JE, Li X, Meng W, Datta A, Bern M, Lim SK, Sze SK. Mol. Cell. Proteomics. 2009; 8(8):1999–2010. [PubMed: 19473960]
23. Pan Y, Stocks BB, Brown L, Konermann L. Anal. Chem. 2009; 81(1):28–35. [PubMed: 19055344]
24. Pan Y, Brown L, Konermann L. J. Mol. Biol. 2009; 394(5):968–981. [PubMed: 19804782]
25. Bavro, Vassiliy N.; Gupta, S.; Ralston, C. Biochem. Soc. Trans. 2015; 43(5):983–994. [PubMed: 26517913]
26. Orban T, Gupta S, Palczewski K, Chance MR. Biochemistry. 2010; 49(5):827–834. [PubMed: 20047303]
27. Angel TE, Gupta S, Jastrzebska B, Palczewski K, Chance MR. Proc. Natl. Acad. Sci. U.S.A. 2009; 106(34):14367–14372. [PubMed: 19706523]
28. Boldog T, Grimme S, Li M, Sligar SG, Hazelbauer GL. Proc. Natl. Acad. Sci. U.S.A. 2006; 103(31):11509–11514. [PubMed: 16864771]
29. Denisov IG, Baas BJ, Grinkova YV, Sligar SG. J. Bio. Chem. 2007; 282(10):7066–7076. [PubMed: 17213193]
30. Bayburt TH, Vishnivetskiy SA, McLean MA, Morizumi T, Huang CC, Tesmer JJG, Ernst OP, Sligar SG, Gurevich VV. J. Biol. Chem. 2011; 286(2):1420–1428. [PubMed: 20966068]
31. Morgan CR, Hebling CM, Rand KD, Stafford DW, Jorgenson JW, Engen JR. Mol. Cell. Proteomics. 2011; 10(9)
32. Parker CH, Morgan CR, Rand KD, Engen JR, Jorgenson JW, Stafford, D W Darrel W. Biochemistry. 2014; 53(9):1511–1520. [PubMed: 24512177]
33. Treuheit NA, Redhair M, Kwon H, McClary WD, Guttman M, Sumida JP, Atkins WM. Biochemistry. 2016; 55(7):1058–1069. [PubMed: 26814638]
34. Cogdell RJ, Fyfe PK, Barrett SJ, Prince SM, Freer AA, Isaacs NW, McGlynn P, Hunter CN. Photosynth. Res. 48(1):55–63.
35. Clayton RK, Clayton BJ. Proc. Natl. Acad. Sci. U.S.A. 1981; 78(9):5583–5587. [PubMed: 16593090]
36. Sligar, SG. http://sligarlab.life.uiuc.edu/nanodisc/protocols.html
37. Gau BC, Sharp JS, Rempel DL, Gross ML. Anal. Chem. 2009; 81(16):6563–6571. [PubMed: 20337372]
38. Consortium, T. U., UniProt: a hub for protein information. Nucleic Acids Res. 2015; 43(D1):D204–D212. [PubMed: 25348405]

39. Tsirigos KD, Peters C, Shu N, Käll L, Elofsson A. The TOPCONS web server for consensus prediction of membrane protein topology and signal peptides. Nucleic Acids Res. 2015
40. Lu Y, Zhang H, Cui W, Saer R, Liu H, Gross ML, Blankenship RE. Biochemistry. 2015; 54(49): 7261–7271. [PubMed: 26574182]
41. Schrödinger, L. New York. The PyMOL Molecular Graphics System, version 1.7.4.
42. Chen XH, Zhang L, Weng YX, Du LC, Ye MP, Yang GZ, Fujii R, Rondonuwu FS, Koyama Y, Wu YS, Zhang JP. Biophys. J. 2005; 88(6):4262–4273. [PubMed: 15821161]
43. Hagn F, Etzkorn M, Raschle T, Wagner G. J. Am. Chem. Soc. 2013; 135(5):1919–1925. [PubMed: 23294159]
44. Inagaki S, Ghirlando R, Grisshammer R. Methods. 2013; 59(3):287–300. [PubMed: 23219517]
45. Inagaki S, Ghirlando R, White JF, Gvozdenovic-Jeremic J, Northup JK, Grisshammer R. J. Mol. Biol. 2012; 417(1–2):95–111. [PubMed: 22306739]
46. Repetto, M.; Boveris, A.; Semprine, J. Lipid peroxidation: chemical mechanism, biological implications and analytical determination. INTECH Open Access Publisher. 2012.
47. Yoon H-H, Lee M-S, Kang J-H. BMB Rep. 2010; 43(3):219–224. [PubMed: 20356464]
48. Niu B, Mackness B, Rempel DL, Zhang Hao, Cui Weidong, Zitzewitz Jill, C Robert Matthews CR, Gross ML. J. Am. Soc. Mass Spectrom. To be submitted.
49. Papiz MZ, Prince SM, Howard T, Cogdell RJ, Isaacs NW. J. Mol. Biol. 2003; 326(5):1523–1538. [PubMed: 12595263]
50. Debnath A, Schäfer LV. J. Phys. Chem. B. 2015; 119(23):6991–7002. [PubMed: 25978497]
51. Bogusz S, Venable RM, Pastor RW. J. Phys. Chem. B. 2000; 104(23):5462–5470.
52. Garavito RM, Ferguson-Miller S. J. Biol. Chem. 2001; 276(35):32403–32406. [PubMed: 11432878]
53. Bond PJ, Cuthbertson J, Sansom MSP. Biochem. Soc. Trans. 2005; 33(5):910–912. [PubMed: 16246008]
54. Bond PJ, Sansom MSP. J. Mol. Biol. 2003; 329(5):1035–1053. [PubMed: 12798692]
55. Kania A, Fiedor L. J. Am. Chem. Soc. 2006; 128(2):454–458. [PubMed: 16402831]
56. Koepke J, Hu X, Muenke C, Schulten K, Michel H. Structure. 1996; 4(5):581–597. [PubMed: 8736556]
57. Singer SJ, Nicolson GL. Science. 1972; 175(4023):720–731. [PubMed: 4333397]
58. Lee AG. Biochim. Biophys. Acta, Biomembr. 2003; 1612(1):1–40.
59. Siuda I, Tieleman DP. J. Chem. Theory Comput. 2015; 11(10):4923–4932. [PubMed: 26574280]
60. Olsen JD, Tucker JD, Timney JA, Qian P, Vassilev C, Hunter CN. J. Biol. Chem. 2008; 283(45): 30772–30779. [PubMed: 18723509]
61. Hennerdal A, Elofsson A. Bioinformatics. 2011; 27(9):1322–1323. [PubMed: 21493661]
62. Gall A, Gardiner AT, Cogdell RJ, Robert B. FEBS Lett. 2006; 580(16):3841–3844. [PubMed: 16790242]
63. Shih AY, Arkhipov A, Freddolino PL, Schulten K. J. Phys. Chem. B. 2006; 110(8):3674–3684. [PubMed: 16494423]
64. Zeng X, Choudhary M, Kaplan S. J. Bacteriol. 2003; 185(20):6171–6184. [PubMed: 14526029]
65. Wang W, Hu Z, Li J, Chen G. Biosci. Rep. 2009; 29(3):165–172. [PubMed: 18798732]
66. Woronowicz K, Olubanjo OB, Sung HC, Lamptey JL, Niederman RA. Photosyn. Res. 2011; 108(2):201–214. [PubMed: 21863386]
67. Espino JA, Mail VS, Jones LM. Anal. Chem. 2015; 87(15):7971–7978. [PubMed: 26146849]

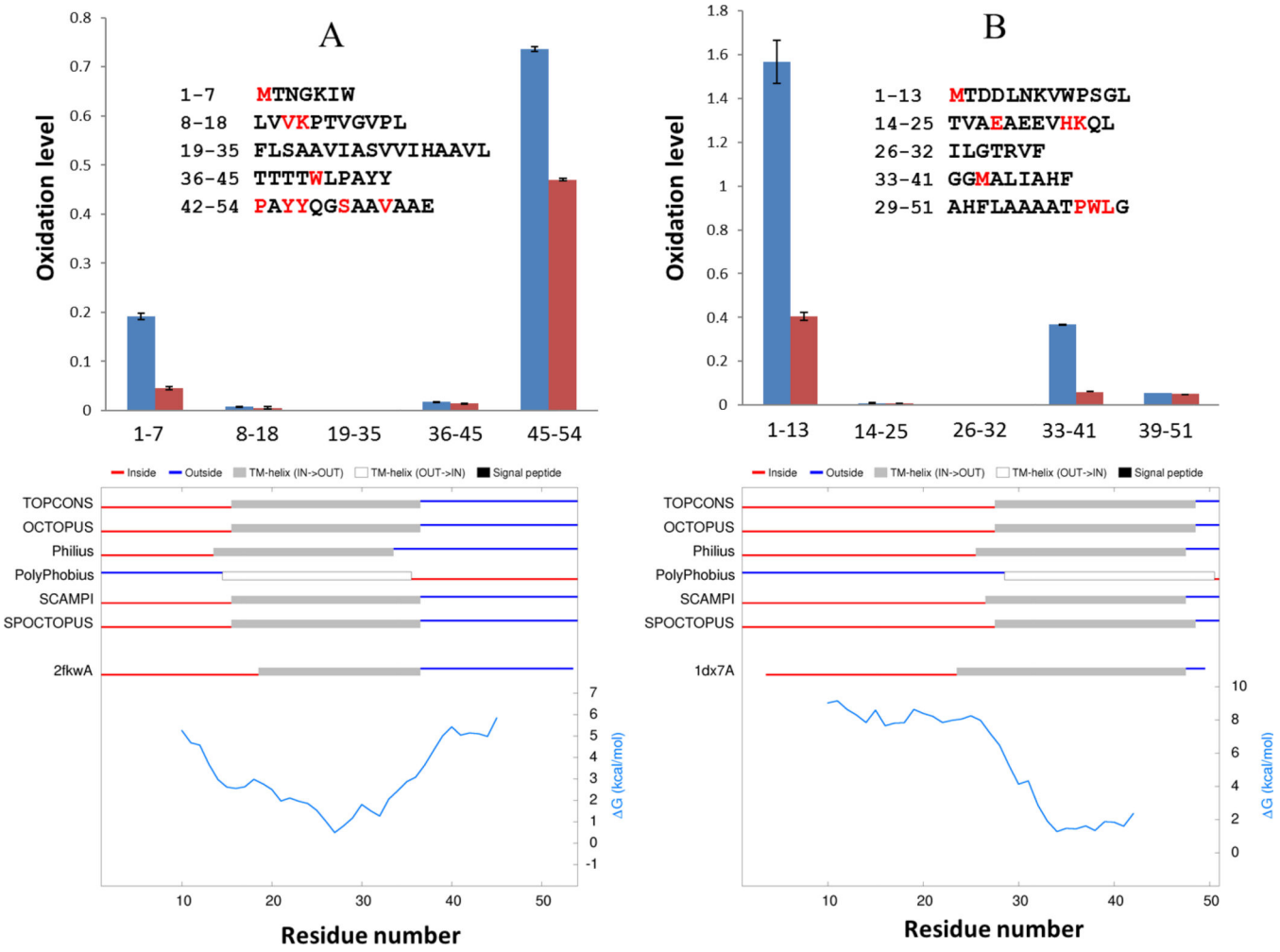

Figure 1.

A. Oxidation levels of α subunit peptides (peptides in detergent are in blue and in Nanodiscs are in red). B. Oxidation level of β1 subunit peptides (Peptides in detergent are in blue, and in Nanodiscs in red). The lower panels in both shows the consensus prediction of membrane protein topology by the TOPCONS web server.

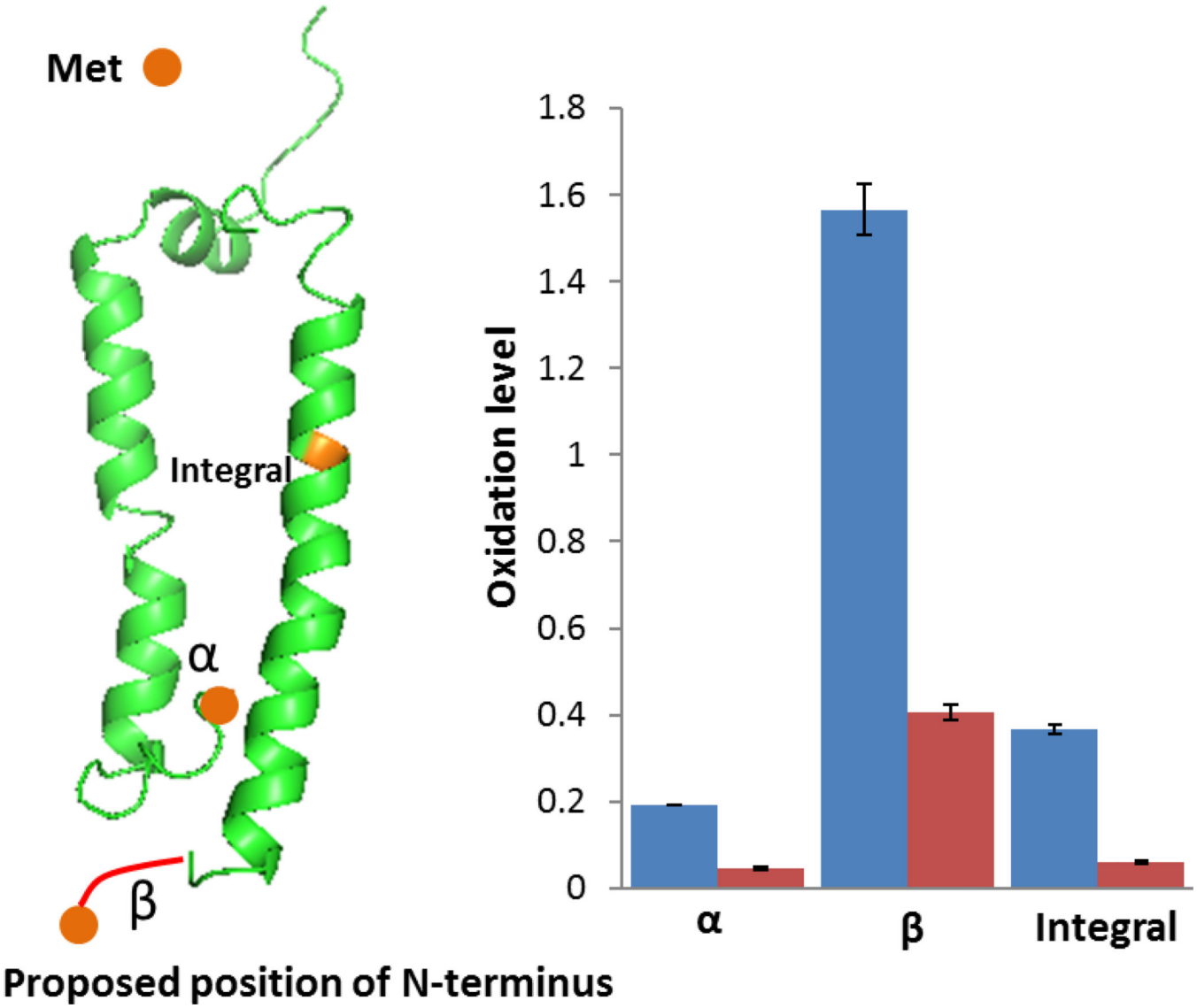

Figure 2.

Oxidation level of Met in detergent micelle/Nanodisc environment. Met are labeled in orange and the proposed positions of Met are shown as orange dots. The proposed N-terminal of β subunit (MTDDLNKVWPSG) is shown as a red line. Results for Mets when the protein is in detergent are in blue; in Nanodiscs in red.

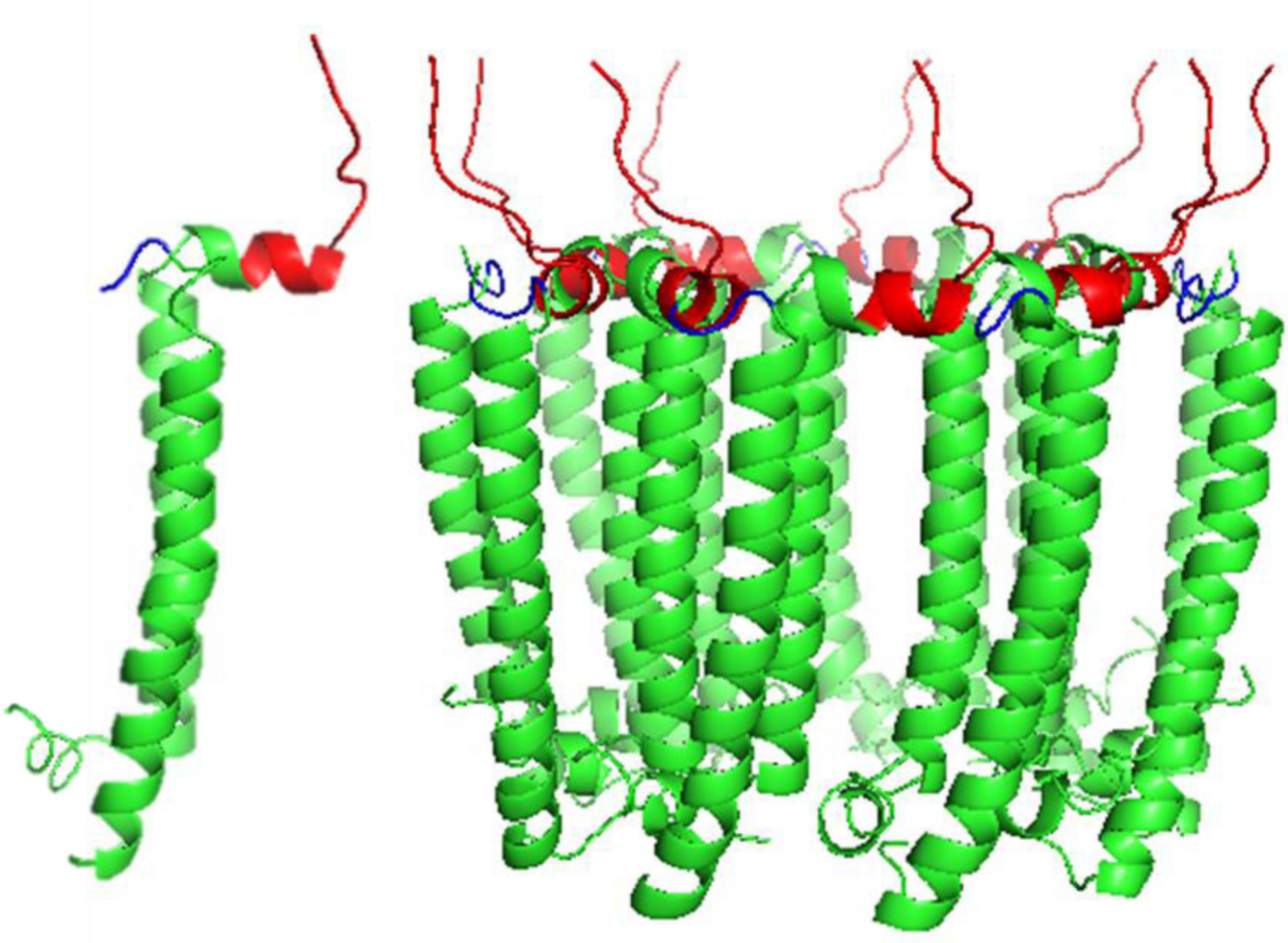

Figure 3.

Peptides on the C-terminal of α subunits are in red in both the homology model (PAYYQGSAAVAAE) and PDB 1NKZ (YWQGGVKKAA). Peptides (PWL) on the C-terminal of β subunits are in blue in both the homology model and PDB 1NKZ. (Full length C-terminal cannot be shown here because it is not covered 100% in the homology model).

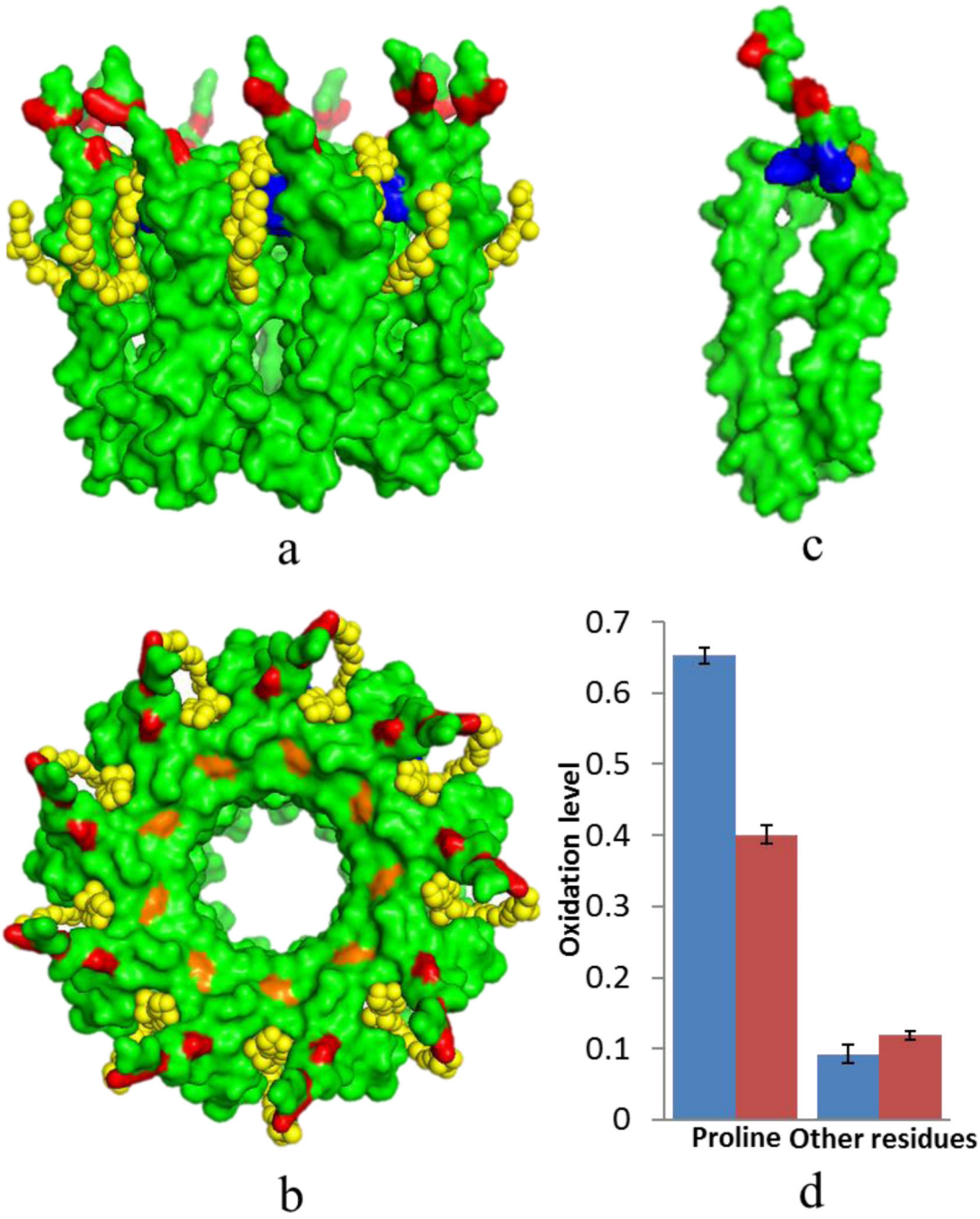

Figure 4.

The homology model (panel c) and PDB 1NKZ (panel a and b) were used to show the residues being discussed in the paper. The second carotenoid (RG2) is shown in yellow as spheres. Prolines in both structures are in orange; Tyr-Try in PDB 1NKZ and the corresponding Tyr-Tyr in homology model are in blue; Gly and Lys in PDB 1NKZ and the corresponding Ser and Val in homology model are in red. Panel d shows the oxidation level of proline vs. other residues. Results from the complex in detergent are in blue, and in Nanodiscs in red.

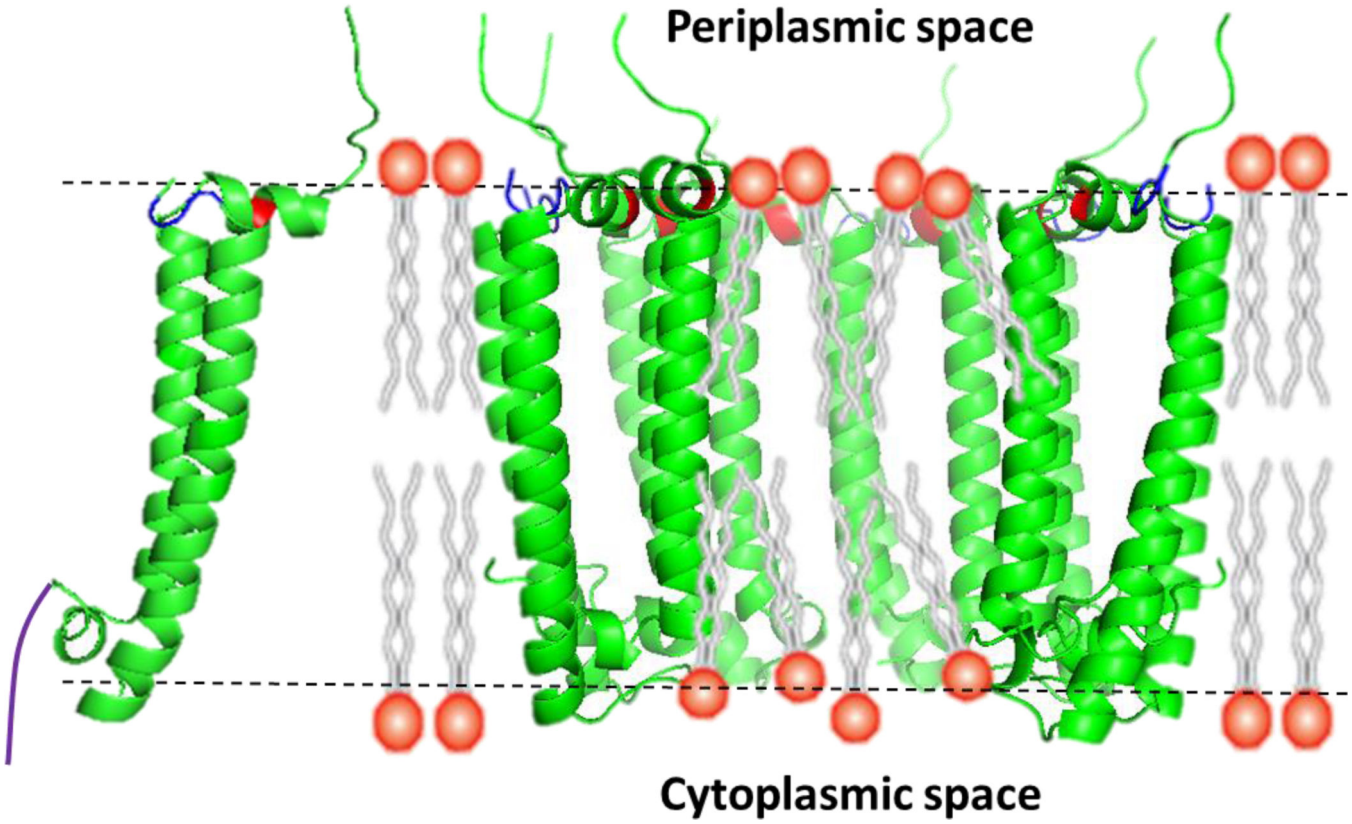

Figure 5.

Proposed borderline between the solvent-accessible domains and the domains embedded in hydrophobic tails of lipids. The heterodimer is shown by the homology model, and the half-ring structure is shown by PDB 1NKZ. The proposed position of β subunit N-terminal (MTDDLNKVWPSG) is in purple in the isolated heterodimer, the proline in C-terminal of α subunit is shown in red and the C-terminal of β subunit is shown in blue. The perturbed lipids packing inside the ring is presented here as cartoon.